

MULTIFIELD VARIATIONAL SECTIONAL ANALYSIS FOR COMPOSITE BLADES BASED ON GENERALIZED TIMOSHENKO-VLASOV THEORY

Manoj Kumar Dhadwal
Konkuk University
Seoul, South Korea

Sung Nam Jung
Konkuk University
Seoul, South Korea

Abstract

A multifield variational finite element (FE) cross-sectional analysis is developed following the Reissner's partially mixed principle for composite blades. The three-dimensional (3D) displacements and cross-sectional dominant stresses are considered to be the primary unknowns in the framework of the multifield principle. The cross-sectional warping deformations due to extensional, transverse shear, bending, and torsional loadings are incorporated. The boundary restraints due to nonuniform torsional warping are modeled to represent end effects for composite beams. The present formulation results in a generalized 7×7 Timoshenko-Vlasov sectional stiffness matrix including elastic couplings. Numerical results for the elastostatic response of composite beams and blades indicate good correlation with the available experimental data and other approaches. In addition, the stresses computed directly from the present multifield approach show an excellent correlation with the 3D FE solutions.

1 INTRODUCTION

The analysis and design of composite blades is a complex task with the cross-section consisting of spar, shear webs, skin, leading edge cap, and foam or honeycomb core regions. With the availability of advanced composites technology, the cross-sectional layup can be tailored for various elastic couplings in order to improve aerodynamic performance and aeroelastic stability, and/or reduce vibration and noise levels. A full 3D analysis of composite blades is usually computationally intensive which inhibits its use for preliminary design and optimization. A vast amount of literature is available on the efficient beam theories including the modeling of composites with various levels of refinements. These beam theories adopt a decomposition approach by overlaying the spanwise cross-sections onto the beam lengthwise reference line [1]. This leads to a two-level analysis: one at a local two-dimensional (2D) sectional level to compute inertial and elastic constants, and the other at a global one-dimensional (1D) level to predict the global static or dynamic behavior [2]. The local sectional analysis is a vital step which involves the modeling of classical elastic couplings combined with nonclassical effects present because of 3D warping displacements and boundary restraints. These effects require careful consideration for accurate determination of sectional elastic characteristics which are then provided as input to 1D beam static or dynamic analyses [3]. The correct recovery of 3D displacements, strains, and stresses is directly linked to the 2D sectional and 1D beam analyses.

Most of the previous works such as in [4, 5] are established based on the displacement formulations implying that the displacements are the primary unknown variables. The strains and stresses are obtained by

differentiation of displacements and applying material constitutive relations which renders those as discontinuous. Although the displacements may be accurately computed using the displacement-based approaches, fairly large number of elements are required to achieve good accuracy for converged stresses. The errors can be significant especially near the restraint region where additional internal loads and stresses may develop due to nonuniform warping. The flexibility and mixed approaches [6] may provide a good alternative which involves modeling of all or in part stress components as unknowns for accurate predictions using fewer elements without the need for displacement derivatives. One such formulation is proposed in the present study.

The present formulation is developed based on the Reissner's multifield variational principle [6]. This work is motivated from the analytical shell-wall based mixed formulation of Jung et al. [3] for composite beams which is based on the Reissner's semi-complementary energy functional. The proposed theory is implemented into a FE program called multifield variational sectional analysis code (MVSAC) which is applicable for nonhomogeneous anisotropic beams with arbitrary geometric shapes and material distributions. The present work has the following unique features: (a) 3D warping displacements and beam sectional stresses (one normal and two transverse shear components; called *reactive stresses* as defined in [6]) are considered as unknowns (field variables). The remaining stress components acting on the planes normal to the cross-section are however computed using the direct constitutive relations and represented in terms of displacement derivatives in the strain relations (called *active stresses* corresponding to the active components); (b) 3D warping displacements (in- and out-of-plane) and beam sectional stresses are obtained

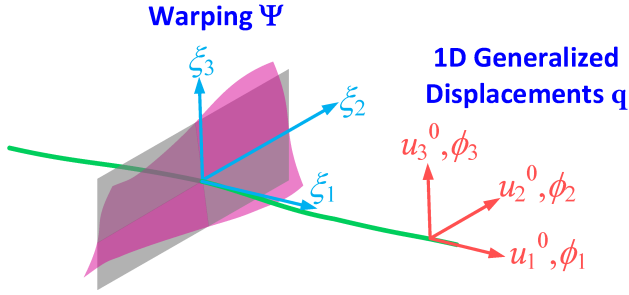


Figure 1: Schematic of beam kinematics indicating cross-sectional warping and 1D generalized displacements.

as part of the analysis which results in a generic non-linear distribution of both 3D warping and reactive stresses over the beam section; (c) the effects of non-uniform torsional warping due to boundary restraints are incorporated resulting in a 7×7 generalized Timoshenko-Vlasov like stiffness model. The present theory also takes into account the classical elastic couplings along with a rigorous treatment of nonclassical couplings due to the transverse shear and Poisson deformations.

2 MULTIFIELD CROSS-SECTIONAL FORMULATION

The schematic of the beam decomposition is shown in Fig. 1 indicating 2D cross-section on the ξ_2 and ξ_3 coordinate plane and 1D reference line aligned along ξ_1 coordinate. The beam is considered to be straight and prismatic. The warping deformation of the 2D beam section, and generalized translational and rotational displacements of the 1D beam reference line are also indicated. The present formulation is valid for prismatic beams with assumptions of small and linear strains at the sectional level and made of linear elastic material.

2.1 Kinematics

The displacements vector \mathbf{u} of an arbitrary material point located on the section of a deformed beam is defined as the sum of the 1D generalized displacements $\mathbf{u}_b = [u_1 \ u_2 \ u_3]^T$ and the 3D warping displacements $\Psi = [\psi_1 \ \psi_2 \ \psi_3]^T$, as given by

$$\mathbf{u} = \mathbf{u}_b + \Psi \quad (1)$$

where

$$\mathbf{u}_b = \mathbf{B}\mathbf{q}, \quad \mathbf{q} = [u_1^0 \ u_2^0 \ u_3^0 \ \phi_1 \ \phi_2 \ \phi_3]^T$$

$$\mathbf{B} = \begin{bmatrix} 1 & 0 & 0 & 0 & \xi_3 & -\xi_2 \\ 0 & 1 & 0 & -\xi_3 & 0 & 0 \\ 0 & 0 & 1 & \xi_2 & 0 & 0 \end{bmatrix} \quad (2)$$

where u_1^0, u_2^0, u_3^0 indicate the translations, and ϕ_1, ϕ_2, ϕ_3 indicate the rotations of the beam section.

The 3D warping displacements in Eq. (1) are six times redundant due to three translations and three rotations of the beam section. The constraints on warping displacements [7] can be applied as

$$\int_A \mathcal{D}_w \Psi \, dA = 0 \quad (3)$$

with A representing the cross-sectional area, and \mathcal{D}_w given as

$$\mathcal{D}_w = \begin{bmatrix} 1 & 0 & 0 \\ 0 & 1 & 0 \\ 0 & 0 & 1 \\ 0 & -\partial_3 & \partial_2 \\ \partial_3 & 0 & -\partial_1 \\ -\partial_2 & \partial_1 & 0 \end{bmatrix} \quad (4)$$

where $\partial_1, \partial_2, \partial_3$ represent the partial derivatives with respect to ξ_1, ξ_2 and ξ_3 , respectively.

With the assumptions of small strains and small local rotations, the linear strains can be obtained in decomposed form as

$$\varepsilon_s^a = \mathbf{B}\Gamma + \mathcal{L}_s^s \Psi + \Psi', \quad \varepsilon_n^a = \mathcal{L}_s^n \Psi \quad (5)$$

where the subscripts s and n respectively represent the sectional stresses and the stresses on the planes normal to the section, and the superscript a represents the active components computed directly from kinematical relations. $\Gamma = [\gamma_1 \ \gamma_2 \ \gamma_3 \ \kappa_1 \ \kappa_2 \ \kappa_3]^T = \mathcal{L}_q \mathbf{q} + \mathbf{q}'$ indicates the generalized strain measures with γ_1 denoting the extensional strain measure, γ_2, γ_3 representing the transverse shear strain measures, κ_1 denoting the twist curvature, and κ_2, κ_3 as the bending curvatures. The terms with $(\cdot)'$ indicate derivatives with respect to ξ_1 , and the matrices $\mathcal{L}_s^s, \mathcal{L}_s^n, \mathcal{L}_q$ are given by

$$\mathcal{L}_s^s = \begin{bmatrix} 0 & 0 & 0 \\ \partial_2 & 0 & 0 \\ \partial_3 & 0 & 0 \end{bmatrix}, \quad \mathcal{L}_s^n = \begin{bmatrix} 0 & \partial_2 & 0 \\ 0 & 0 & \partial_3 \\ 0 & \partial_3 & \partial_2 \end{bmatrix}$$

$$\mathcal{L}_q = \begin{bmatrix} 0 & 0 & 0 & 0 & 0 & 0 \\ 0 & 0 & 0 & 0 & 0 & -1 \\ 0 & 0 & 0 & 0 & 1 & 0 \\ 0 & 0 & 0 & 0 & 0 & 0 \\ 0 & 0 & 0 & 0 & 0 & 0 \\ 0 & 0 & 0 & 0 & 0 & 0 \end{bmatrix} \quad (6)$$

The warping and reactive stress fields are discretized at 2D sectional level as

$$\Psi(\xi_1, \xi_2, \xi_3) = \mathbf{N}_\psi(\xi_2, \xi_3)\Lambda(\xi_1)$$

$$\sigma_s^r(\xi_1, \xi_2, \xi_3) = \mathbf{N}_\sigma(\xi_2, \xi_3)\Upsilon(\xi_1) \quad (7)$$

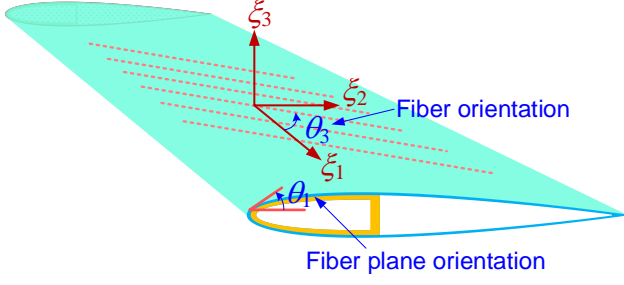


Figure 2: Material orientations.

where $\mathbf{N}_\psi(\xi_2, \xi_3)$ and $\mathbf{N}_\sigma(\xi_2, \xi_3)$ represent the FE shape function matrices respectively for the warping and reactive stress fields, and $\Lambda(\xi_1)$ and $\Upsilon(\xi_1)$ indicate the corresponding nodal values of warping and reactive stress fields.

The warping constraints in Eq. (3) can be discretized using Eq. (7) as

$$\int_A \mathcal{D}_w \mathbf{N}_\psi \Lambda dA = \left(\int_A \mathcal{D}_w \mathbf{N}_\psi dA \right) \Lambda = \mathbf{D}_\psi \Lambda = \mathbf{0} \quad (8)$$

where \mathbf{D}_ψ denotes the discretized warping constraints matrix.

2.2 Semi-inverted Material Constitutive Relations

For a generally anisotropic linear elastic material, the material constitutive relations can be expressed using generalized Hooke's law as given by

$$\sigma_m = \mathbf{C}_m \varepsilon_m \quad (9)$$

where σ_m denotes the stress vector, ε_m denotes the strain vector, and \mathbf{C}_m represents the material constitutive matrix. The constitutive relations in the material coordinate system are transformed to the beam coordinate system through consecutive rotations by fiber angle θ_3 and fiber plane angle θ_1 indicated in Fig. 2.

For the multifield formulation, the stresses and strains are decomposed into sectional stresses acting on the beam section (normal and transverse shear stresses) and stresses acting on the planes normal to the beam section (normal and in-plane shear stresses). The semi-inverted form of constitutive relations is then expressed as

$$\begin{Bmatrix} \varepsilon_s^r \\ \sigma_n^a \end{Bmatrix} = \begin{bmatrix} \bar{\mathbf{C}}_{ss} & \bar{\mathbf{C}}_{sn} \\ -\bar{\mathbf{C}}_{sn}^T & \bar{\mathbf{C}}_{nn} \end{bmatrix} \begin{Bmatrix} \sigma_s^r \\ \varepsilon_n^a \end{Bmatrix} \quad (10)$$

where the superscript r denotes the reactive components and the superscript a indicates the stresses computed from the strains using Hooke's law.

2.3 Governing Equations

The present formulation assumes sectional normal and transverse shear stresses to be unknowns along with the displacements which are modeled through a variational principle leading to a *multifield variational formulation*. The variation of total energy per unit beam length $\delta\Pi_R$ is stated as

$$\delta\Pi_R = \delta U_s - \delta W_s = \delta L \quad (11)$$

where δU_s and δW_s respectively indicate the variations of cross-sectional strain energy and external work per unit beam length. The term δL denotes the variation of warping constraints which can be obtained from Eq. (8) using Lagrange multipliers Θ_ψ as

$$\delta L = -\delta \left((\mathbf{D}_\psi \Lambda)^T \Theta_\psi \right) = -\delta \Lambda^T \mathbf{D}_\psi^T \Theta_\psi - \delta \Theta_\psi^T (\mathbf{D}_\psi \Lambda) \quad (12)$$

The Reissner's semi-complementary energy functional Φ_R [6] can be defined in a generalized form as

$$\Phi_R = \frac{1}{2} \left((\varepsilon_n^a)^T \sigma_n^a - (\sigma_s^r)^T \varepsilon_s^r \right) \quad (13)$$

The sectional strain energy U_s is obtained using Reissner's semi-complementary energy functional Φ_R [6] as

$$U_s = \int_A [\Phi_R + (\varepsilon_s^r)^T \sigma_s^r] dA \quad (14)$$

The reactive strains ε_s^r computed using semi-inverted material constitutive relations in Eq. 10 and the active strains ε_n^a computed from the kinematics must satisfy the compatibility condition implying $\varepsilon_s^r = \varepsilon_s^a$. Substituting Φ_R from Eq. (13), the first variation of the sectional strain energy is then obtained as

$$\delta U_s = \int_A \left[(\delta \varepsilon_n^a)^T \sigma_n^a + (\delta \varepsilon_s^a)^T \sigma_s^r + (\delta \sigma_s^r)^T (\varepsilon_s^a - \varepsilon_s^r) \right] dA \quad (15)$$

Substituting Eqs. (10), (5) and (7) into the above equation, the sectional strain energy variation can be written in matrix form as

$$\delta U_s = \begin{Bmatrix} \delta \Lambda' \\ \delta \Upsilon \\ \delta \Lambda \\ \delta \Gamma \\ \delta \Theta_\psi \end{Bmatrix}^T \begin{bmatrix} \mathbf{0} & \mathbf{A} & \mathbf{0} & \mathbf{0} & \mathbf{0} \\ \mathbf{A}^T & -\mathbf{H} & \mathbf{G}^T & \mathbf{R} & \mathbf{0} \\ \mathbf{0} & \mathbf{G} & \mathbf{E} & \mathbf{0} & \mathbf{0} \\ \mathbf{0} & \mathbf{R}^T & \mathbf{0} & \mathbf{0} & \mathbf{0} \\ \mathbf{0} & \mathbf{0} & \mathbf{0} & \mathbf{0} & \mathbf{0} \end{bmatrix} \begin{Bmatrix} \Lambda' \\ \Upsilon \\ \Lambda \\ \Gamma \\ \Theta_\psi \end{Bmatrix} \quad (16)$$

where

$$\begin{aligned} \mathbf{A} &= \int_A \mathbf{N}_\psi^T \mathbf{N}_\sigma dA, & \mathbf{E} &= \int_A (\mathcal{L}_s^n \mathbf{N}_\psi)^T \bar{\mathbf{C}}_{nn} \mathcal{L}_s^n \mathbf{N}_\psi dA \\ \mathbf{G} &= \int_A (\mathcal{L}_s^s \mathbf{N}_\psi - \bar{\mathbf{C}}_{sn} \mathcal{L}_s^n \mathbf{N}_\psi)^T \mathbf{N}_\sigma dA \\ \mathbf{H} &= \int_A \mathbf{N}_\sigma^T \bar{\mathbf{C}}_{ss} \mathbf{N}_\sigma dA, & \mathbf{R} &= \int_A \mathbf{N}_\sigma^T \mathbf{B} dA \end{aligned} \quad (17)$$

The submatrices \mathbf{A} , \mathbf{E} , \mathbf{G} , \mathbf{H} , and \mathbf{R} describe the geometric and material coupling effects of the beam section.

The sectional stress resultants \mathbf{F} are defined using the tractions σ_s acting on the section as given by

$$\mathbf{F} = \int_A \mathbf{B}^T \sigma_s dA \quad (18)$$

with

$$\mathbf{F} = [F_1 \ F_2 \ F_3 \ M_1 \ M_2 \ M_3]^T \quad (19)$$

where F_1 is the extensional force, F_2 and F_3 are the transverse shear forces, M_1 is the torsional moment, and M_2 and M_3 are the bending moments.

Assuming negligible surface and body forces, the external work per unit length of the beam W_s is given by

$$W_s = \int_A (\mathbf{u}^T \sigma_s)' dA \quad (20)$$

Using Eqs. (1), (2), and Eq. (18), and substituting the discretized warping and reactive stress fields from Eq. (7), the variation of external work δW_s becomes

$$\delta W_s = \begin{Bmatrix} \delta \Lambda' \\ \delta \Upsilon \\ \delta \Lambda \\ \delta \Gamma \\ \delta \Theta_\psi \end{Bmatrix}^T \begin{Bmatrix} \mathbf{P} \\ \mathbf{0} \\ \mathbf{P}' \\ \mathbf{F} \\ \mathbf{0} \end{Bmatrix} + \delta \mathbf{q}^T (\mathbf{F}' - \mathcal{L}_q^T \mathbf{F}) \quad (21)$$

where

$$\mathbf{P} = \int_A \mathbf{N}_\psi^T \sigma_s dA, \quad \mathbf{P}' = \int_A \mathbf{N}_\psi^T (\sigma_s)' dA \quad (22)$$

Substituting Eqs. (16), (21) and (12) in Eq. (11), and considering double derivatives of warping and reactive stresses with respect to ξ_1 to be zero, the equilibrium equations for a unit beam length can be formulated as

$$\begin{bmatrix} -\mathbf{H} & \mathbf{G}^T & \mathbf{R} & \mathbf{0} \\ \mathbf{G} & \mathbf{E} & \mathbf{0} & \mathbf{D}_\psi^T \\ \mathbf{R}^T & \mathbf{0} & \mathbf{0} & \mathbf{0} \\ \mathbf{0} & \mathbf{D}_\psi & \mathbf{0} & \mathbf{0} \end{bmatrix} \begin{Bmatrix} \Upsilon' \\ \Lambda' \\ \Gamma' \\ \Theta'_\psi \end{Bmatrix} = \begin{Bmatrix} \mathbf{0} \\ \mathbf{0} \\ \mathcal{L}_q^T \mathbf{F} \\ \mathbf{0} \end{Bmatrix} \quad (23a)$$

$$\begin{bmatrix} -\mathbf{H} & \mathbf{G}^T & \mathbf{R} & \mathbf{0} \\ \mathbf{G} & \mathbf{E} & \mathbf{0} & \mathbf{D}_\psi^T \\ \mathbf{R}^T & \mathbf{0} & \mathbf{0} & \mathbf{0} \\ \mathbf{0} & \mathbf{D}_\psi & \mathbf{0} & \mathbf{0} \end{bmatrix} \begin{Bmatrix} \Upsilon \\ \Lambda \\ \Gamma \\ \Theta_\psi \end{Bmatrix} = \begin{bmatrix} \mathbf{0} & -\mathbf{A}^T & \mathbf{0} & \mathbf{0} \\ \mathbf{A} & \mathbf{0} & \mathbf{0} & \mathbf{0} \\ \mathbf{0} & \mathbf{0} & \mathbf{0} & \mathbf{0} \\ \mathbf{0} & \mathbf{0} & \mathbf{0} & \mathbf{0} \end{bmatrix} \begin{Bmatrix} \Upsilon' \\ \Lambda' \\ \Gamma' \\ \Theta'_\psi \end{Bmatrix} + \begin{Bmatrix} \mathbf{0} \\ \mathbf{0} \\ \mathbf{F} \\ \mathbf{0} \end{Bmatrix} \quad (23b)$$

The warping displacements and reactive stresses are considered to be linear functions of sectional stress resultants, expressed as

$$\begin{aligned} \Lambda &= \tilde{\Lambda} \mathbf{F}, \quad \Upsilon = \tilde{\Upsilon} \mathbf{F}, \quad \Gamma = \tilde{\Gamma} \mathbf{F}, \quad \Theta_\psi = \tilde{\Theta}_\psi \mathbf{F} \\ \Lambda' &= \tilde{\Lambda}_p \mathbf{F}, \quad \Upsilon' = \tilde{\Upsilon}_p \mathbf{F}, \quad \Gamma' = \tilde{\Gamma}_p \mathbf{F}, \quad \Theta'_\psi = \tilde{\Theta}_{\psi p} \mathbf{F} \end{aligned} \quad (24)$$

where $\tilde{\Lambda}$ and $\tilde{\Upsilon}$ represent the nodal values of warping and reactive stress coefficients, and $\tilde{\Gamma}$ indicate the strain measure coefficient matrix which is constant over the beam section. The matrices $\tilde{\Theta}_\psi$ and $\tilde{\Theta}_{\psi p}$ represent the Lagrange multiplier coefficients for consistency sake. The terms with subscript p indicate the coefficients corresponding to the derivative of generalized strain measures present in the sectional stress resultants. The coefficient matrices include contributions from extension, transverse shear, bending, and torsion, and these describe a nonlinear distribution over the beam section. The warping and reactive stress coefficients are solved by substituting in the equilibrium equations obtained in Eq. (23). These coefficient matrices are later used to accurately compute the sectional stiffness constants including any elastic couplings.

2.4 Generalized Timoshenko-Vlasov Stiffness Matrix

The generalized Timoshenko like 6×6 stiffness matrix is first constituted using the Saint-Venant warping which is assumed as uniform along the beam axis. With the known warping solution from Eq. (23), the strain energy variation (δU_s) from Eq. (16) becomes

$$\delta U_s = \delta \mathbf{F}^T \begin{bmatrix} \tilde{\Lambda}_p \\ \tilde{\Upsilon} \\ \tilde{\Lambda} \\ \tilde{\Gamma} \end{bmatrix}^T \begin{bmatrix} \mathbf{0} & \mathbf{A} & \mathbf{0} & \mathbf{0} \\ \mathbf{A}^T & -\mathbf{H} & \mathbf{G}^T & \mathbf{R} \\ \mathbf{0} & \mathbf{G} & \mathbf{E} & \mathbf{0} \\ \mathbf{0} & \mathbf{R}^T & \mathbf{0} & \mathbf{0} \end{bmatrix} \begin{bmatrix} \tilde{\Lambda}_p \\ \tilde{\Upsilon} \\ \tilde{\Lambda} \\ \tilde{\Gamma} \end{bmatrix} \mathbf{F} \quad (25)$$

The variation of the external work can be restated in terms of Timoshenko like sectional flexibility matrix \mathbf{S}_T as

$$\delta W_s = \delta \Gamma^T \mathbf{F} = \delta \mathbf{F}^T \mathbf{S}_T \mathbf{F} \quad (26)$$

where \mathbf{S}_T can be determined using energy principle defined in Eq. (11), which results in

$$\mathbf{S}_T = \begin{bmatrix} \tilde{\Lambda}_p \\ \tilde{\Upsilon} \\ \tilde{\Lambda} \\ \tilde{\Gamma} \end{bmatrix}^T \begin{bmatrix} \mathbf{0} & \mathbf{A} & \mathbf{0} & \mathbf{0} \\ \mathbf{A}^T & -\mathbf{H} & \mathbf{G}^T & \mathbf{R} \\ \mathbf{0} & \mathbf{G} & \mathbf{E} & \mathbf{0} \\ \mathbf{0} & \mathbf{R}^T & \mathbf{0} & \mathbf{0} \end{bmatrix} \begin{bmatrix} \tilde{\Lambda}_p \\ \tilde{\Upsilon} \\ \tilde{\Lambda} \\ \tilde{\Gamma} \end{bmatrix} \quad (27)$$

The generalized 6×6 Timoshenko like stiffness matrix \mathbf{K}_T can be computed by inverting the flexibility matrix, which implies $\mathbf{K}_T = \mathbf{S}_T^{-1}$. The stiffness matrix \mathbf{K}_T takes into account the effects of elastic couplings, transverse shear, and Poisson deformation. For the case of general anisotropic beams, the 6×6 stiffness matrix may be fully populated.

In order to account for the boundary effect due to non-uniform torsion for open section beams, the torsional

warping stiffness and related coupling stiffness constants must be computed. To this end, torsional bimoment M_{w1} is introduced following Vlasov's theory [8]. The sectional stress resultants $\hat{\mathbf{F}}$ and corresponding generalized strain measures $\hat{\Gamma}$ for the Timoshenko-Vlasov model are then defined as

$$\hat{\mathbf{F}} = \begin{bmatrix} \mathbf{F}^T & M_{w1} \end{bmatrix}^T, \quad \hat{\Gamma} = \begin{bmatrix} \Gamma^T & \kappa'_1 \end{bmatrix}^T \quad (28)$$

The sectional strain energy variation for the generalized Timoshenko-Vlasov model is derived to include the warping dependent strain energy in addition to the generalized Timoshenko level strain energy given in Eq. (16), which leads to

$$\delta U_s = \delta U_s^{GT} + \delta U_s^W \quad (29)$$

where δU_s^{GT} is the contribution from the generalized Timoshenko model, and δU_s^W is the contribution from the nonuniform warping, respectively given by

$$\begin{aligned} \delta U_s^{GT} &= \delta \Gamma^T \mathbf{K} \Gamma \quad (30) \\ \delta U_s^W &= \begin{Bmatrix} \delta \Lambda' \\ \delta \Lambda \end{Bmatrix}^T \begin{bmatrix} \mathbf{A}\mathbf{H}^{-1}\mathbf{A}^T & \mathbf{A}\mathbf{H}^{-1}\mathbf{G}^T \\ (\mathbf{A}\mathbf{H}^{-1}\mathbf{G}^T)^T & (\mathbf{E} + \mathbf{G}\mathbf{H}^{-1}\mathbf{G}^T) \end{bmatrix} \begin{Bmatrix} \Lambda' \\ \Lambda \end{Bmatrix} \\ &\quad + \begin{Bmatrix} \delta \Lambda' \\ \delta \Lambda \end{Bmatrix}^T \begin{bmatrix} \mathbf{A}\mathbf{H}^{-1}\mathbf{R} \\ \mathbf{G}\mathbf{H}^{-1}\mathbf{R} \end{bmatrix} \Gamma + \delta \Gamma^T \begin{bmatrix} \mathbf{A}\mathbf{H}^{-1}\mathbf{R} \\ \mathbf{G}\mathbf{H}^{-1}\mathbf{R} \end{bmatrix}^T \begin{Bmatrix} \Lambda' \\ \Lambda \end{Bmatrix} \quad (31) \end{aligned}$$

The nodal reactive stresses Υ are expressed in terms of warping displacements (Λ), their derivatives (Λ'), and generalized strain measures (Γ). For the generalized Timoshenko-Vlasov model, only the derivative of torsional strain measure (κ'_1) will be required to represent the nonuniform distribution along the beam span. The generalized Timoshenko model readily takes into account the warping displacements without derivatives. The expression for the variation of warping-dependent strain energy can be reduced using a static condensation procedure which involves the elimination of diagonal coupling terms defined in Eq. (31).

For the generalized Timoshenko-Vlasov model, the nodal warping displacements (Λ) and their derivatives (Λ') are expressed in terms of generalized strain measures (Γ) using generalized Timoshenko stiffness matrix \mathbf{K}_T , which implies

$$\Lambda = \hat{\Lambda}\Gamma, \quad \Lambda' = \hat{\Lambda}'\Gamma', \quad \hat{\Lambda} = \tilde{\Lambda}\mathbf{K}_T \quad (32)$$

where $\tilde{\Lambda}$ is the warping coefficient matrix corresponding to generalized stress resultants obtained from Eq. (23), and $\hat{\Lambda}$ is the modified warping coefficients matrix corresponding to the generalized strain measures Γ .

Using the above relations and retaining only the derivative of nonzero torsional strain measure, the variation of the total sectional strain energy (δU_s) from Eq. (29) is updated as

$$\delta U_s = \begin{Bmatrix} \delta \Gamma \\ \delta \kappa'_1 \end{Bmatrix}^T \begin{bmatrix} \mathbf{K}_T & \mathbf{K}_{TW} \\ \mathbf{K}_{TW}^T & K_W \end{bmatrix} \begin{Bmatrix} \Gamma \\ \kappa'_1 \end{Bmatrix} \quad (33)$$

where K_W is the torsional warping stiffness and the vector \mathbf{K}_{TW} consists of torsional warping related coupling coefficients.

The variation of external work for the generalized Timoshenko-Vlasov model can be accordingly redefined as

$$\delta W_s = \delta \hat{\Gamma}^T \hat{\mathbf{F}} = \delta \hat{\Gamma}^T \mathbf{K} \hat{\Gamma} \quad (34)$$

where \mathbf{K} is a 7×7 Timoshenko-Vlasov like stiffness matrix which can be determined using the variational principle defined in Eq. (11) resulting in

$$\mathbf{K} = \begin{bmatrix} \mathbf{K}_T & \mathbf{K}_{TW} \\ \mathbf{K}_{TW}^T & K_W \end{bmatrix} \quad (35)$$

The additional stiffness coefficients \mathbf{K}_{TW} and K_W in the above equation represent the nonuniform torsional warping effect due to the presence of boundary restraints.

3 VALIDATION RESULTS

The present multifield formulation is implemented into a FE analysis called MVSAC. Several composite beams and blades are presented to substantiate the efficacy of the present analysis in comparison to 3D FE solutions and/or experimental data. The 3D warping deformation modes and 1D elastostatic response are presented for elastically coupled blades and beams. The influence of nonuniform torsional warping on the elastostatic response is demonstrated for open-section composite I-beams. The sample results on the recovery of sectional stresses are also presented for thin laminated strips.

3.1 Two-cell Composite Blades

Two-cell composite blades originally studied by Chandra and Chopra [9, 10] are considered first. Figure 3 shows the geometric and material layup of the blade section. The outer profile of the blade section is that of NACA 0012 airfoil with a chord length (c) of 3 in. The blade has an effective length of 25.25 in excluding the clamped root end. The blade is made of graphite-epoxy material with the properties given as [10]: $E_{11} = 19 \times 10^6$ psi, $E_{22} = E_{33} = 1.35 \times 10^6$ psi, $G_{12} = G_{13} = G_{23} = 0.85 \times 10^6$ psi, and $\nu_{12} = \nu_{13} = \nu_{23} = 0.4$. The blade exhibits bending-torsion and extension-shear couplings due to angle ply configurations. The fiber angle θ is varied as 15, 30, and 45 degrees. The blade section is discretized using 2,760 eight-node quadrilateral elements and 9,159 nodes leading to a total of 54,954 degrees of freedom.

Figure 4 presents the warping displacement modes for composite blade with fiber angle having 45 degrees.

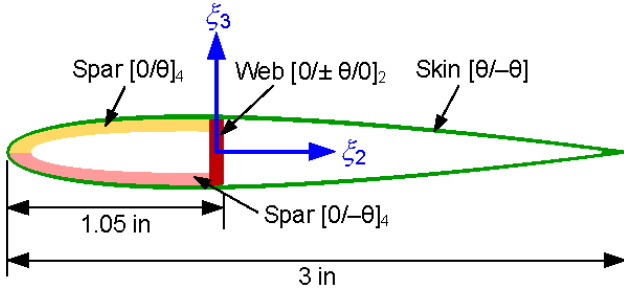


Figure 3: Composite blade with bending-torsion coupling.

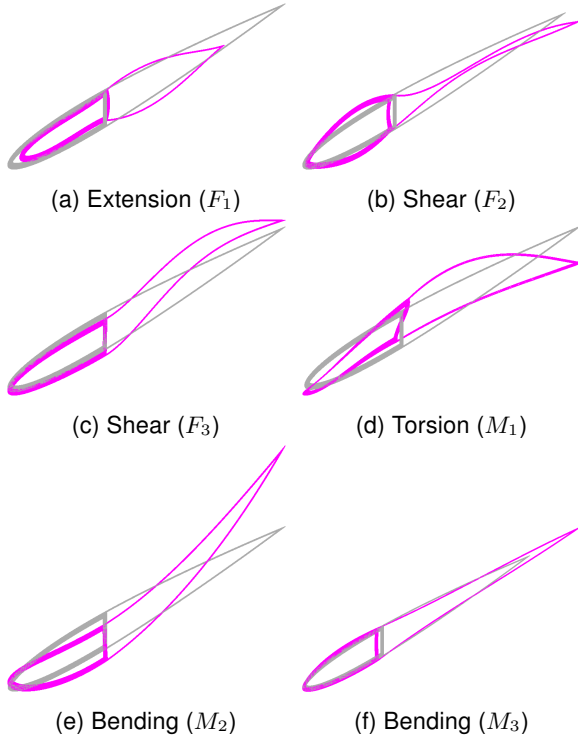


Figure 4: Warping displacement modes of bending-torsion coupled composite blades with $\theta = 45$ deg (exaggerated).

The extensional mode depicted in Fig. 4a shows out-of-plane deformation due to coupling with the shear mode. The bending mode in Fig. 4e indicates out-of-plane deformation due to coupling with the torsional mode. The determination of these couplings affects the prediction of global behavior of composite blades.

Next, the 1D elastostatic response of cantilevered composite blades is investigated under the application of a tip shear force of 1 lb. The torsional warping is restrained at both the root and tip ends. Because of the bending-torsion coupling, twist will be induced due to the tip shear force. The present results are compared with the experimental results of Chandra and Chopra [9, 10], and Jung and Park [11]. Reference 11 followed a mixed analytical approach to compute the sectional elastic constants. Figure 5 presents the com-

parison of tip bending slope and tip induced twist under a tip shear force. The present multifield MVSAC shows an excellent correlation for both tip bending slope and tip induced twist with the exception of tip induced twist at 15 deg fiber angle. The present predictions are very close to those of displacement-based RDSAC and are reported to be better than Jung and Park [11]. Overall, a better correlation is achieved compared to that of analytical results of Ref. 11 and displacement-based FE analysis RDSAC. Note that the present MVSAC accurately describes the geometric layout and composite material distribution using 2D FEs as opposed to a shell-wall contour based analytical approach adopted in Ref. 11. It is remarked that Ref. 11 follows the zero hoop stress flow assumption whereas the present approach does not make any such ad-hoc assumptions. It is observed that the present multifield-based MVSAC clearly achieves improved correlation with the experimental data for elastically coupled composite blades.

3.2 Composite I-beam

An open-section composite I-beam [9] with a symmetric layup is considered, as shown in Fig. 6. The cross-section exhibits bending-torsion and extension-shear couplings. The material properties can be found in [9]. The section is discretized using 400 eight-node quadrilateral elements and 1,333 nodes.

The warping deformation modes are illustrated in Fig. 7. The extension-shear coupling can be seen for extension (F_1) mode indicating out-of-plane deformation due to coupling with shear (F_2) mode. The bending-torsion coupling leads to an additional out-of-plane deformation in the bending (M_2) mode with similar profile as that of torsion (M_1) mode. Little extension-bending coupling can also be observed in the bending (M_3) mode deformation.

The 1D elastostatic torsional response is computed next for a cantilever beam with length L as 0.762 m. The cross-sectional warping is restrained at the tip end where a torsional moment (M_1) of 0.113 N m is applied. Fig. 8 presents the comparison of the twist response computed using the present analysis MVSAC with those of Nastran 3D FE solutions, experimental data [9], Jung et al. [3], and displacement-based analysis RDSAC [7]. The present results show good correlation with both the experimental data [9] and Nastran 3D FE solutions. The twist angle in Fig. 8a shows a maximum difference of 6.11 % compared to 3D Nastran near the tip end. The difference in tip twist between the present MVSAC and the displacement-based RDSAC [7] is less than 3 %. The twist rate presented in Fig. 8b also correlates well with 3D Nastran solution. The influence of the warping restraint

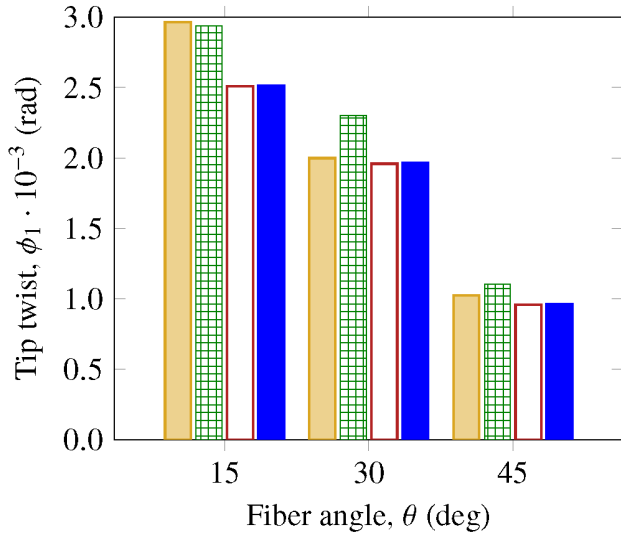
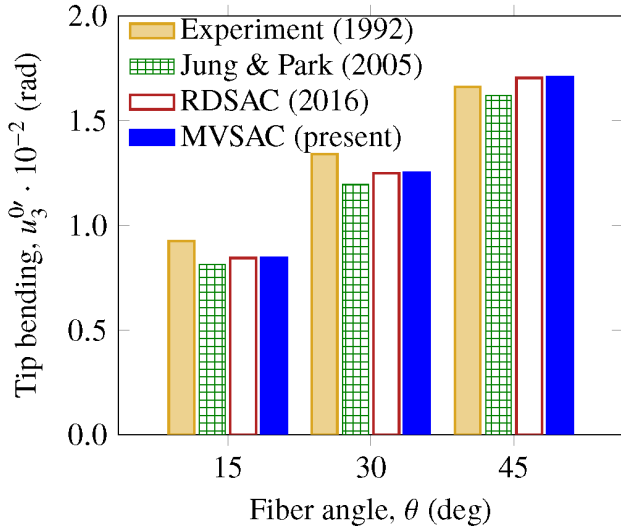


Figure 5: (a) Tip bending slope and (b) tip induced twist of composite blades under a tip shear force.

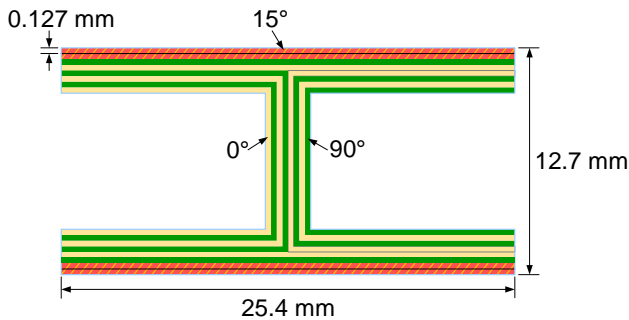


Figure 6: Composite I-beam.

on the twist response is clearly visible at the tip end of the composite I-beam where the twist rate approaches zero.

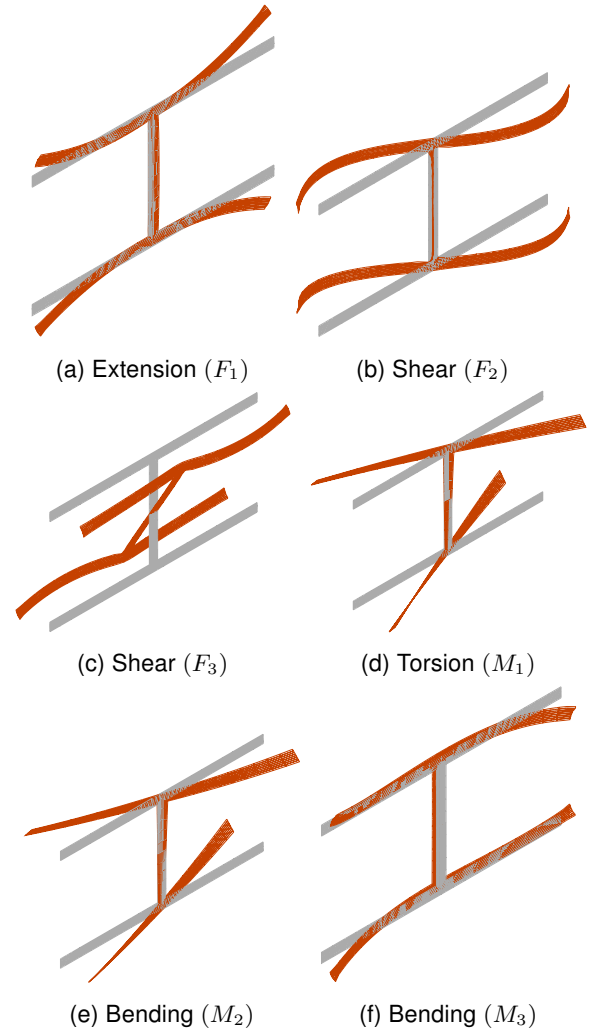
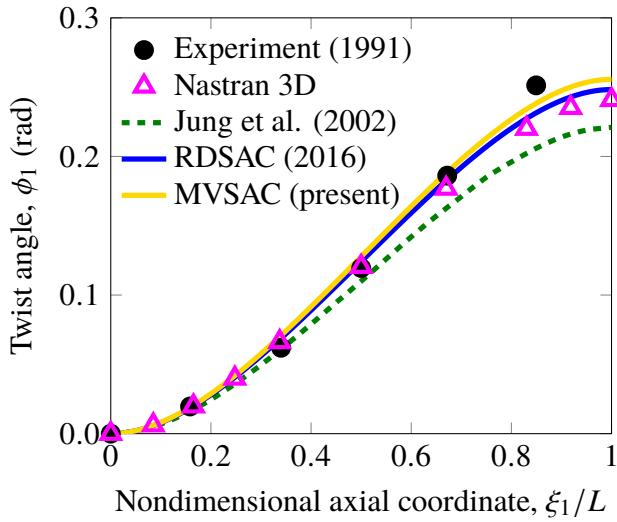


Figure 7: Warping modes for composite I-beam (exaggerated).

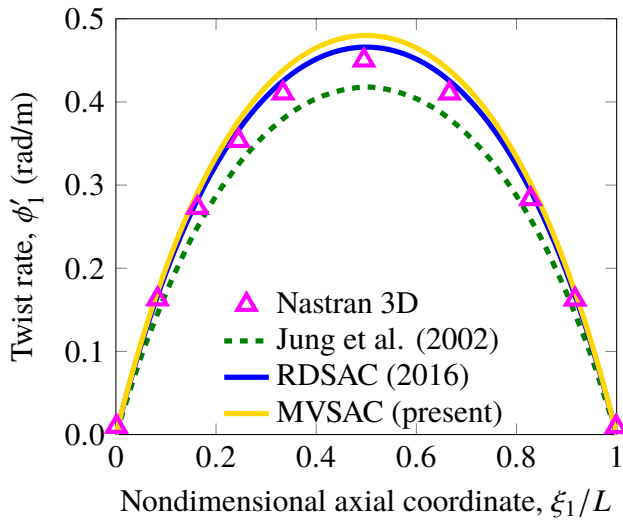
3.3 Thin Laminated Strip

In order to illustrate the stress recovery, a thin laminated strip is considered taken from Liu and Yu [12]. The strip is 0.04 m thick, 0.18 m wide, and 1 m long with a cross-ply layup of $[90/0]_2$. The beam is cantilevered at the root end and an extensional force F_1 of 10 kN is applied at the tip end. The strip section is modeled using 2,560 eight-node quadrilateral elements and 7,905 nodes.

Figure 9 presents the comparison of the normal stress, along the strip thickness at the mid-span ($\xi_1 = 0.5$ m), computed by the present MVSAC with those of 3D FE solutions [12] and mechanics of structure genome (MSG) approach [12]. Since the strip is composed of four layers, the stress discontinuity is well captured by the present analysis. The present stress values show excellent correlation with the 3D FE solutions which are indistinguishable in the plot. The present analysis computes these stresses directly without requiring



(a) Twist angle ϕ_1



(b) Twist rate ϕ'_1

Figure 8: Torsional response of composite I-beam under tip torsional moment.

displacement derivatives while maintaining the stress continuity within the composite layer and discontinuity at the layer boundaries.

4 CONCLUDING REMARKS

A multifield variational sectional analysis is developed taking into account the classical elastic couplings as well as the nonclassical torsional warping restraint. Both 3D warping displacements and reactive sectional stresses are computed as part of the analysis through the application of multifield variational principle which leads to accurate prediction of stiffness constants as well as stresses. A Timoshenko-Vlasov like 7×7 stiffness matrix is derived from the formulation. The present results are validated for thin-walled beams and

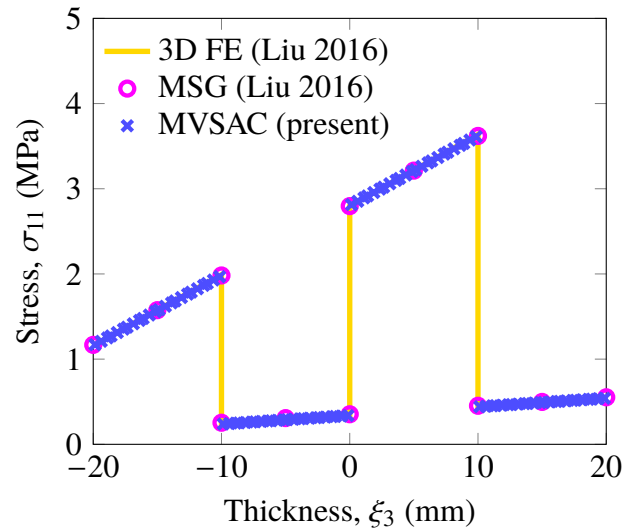


Figure 9: Normal stress σ_{11} for thin laminated strip under an extensional force.

blades with elastic couplings. The elastostatic responses of composite blade and I-beam computed by the present multifield-based MVSAC demonstrate a good correlation with the experimental data and 3D FE solutions. The recovery of sectional normal stress is illustrated for a thin laminated beam which is almost identical to the 3D FE solution. These sectional stresses are directly recovered from the reactive stress coefficients while maintaining stress discontinuity at the layer interfaces. The present analysis clearly demonstrates the application for composite rotor blades with elastic couplings along with the recovery of sectional stresses through the proposed multifield-based reactive stress coefficients.

ACKNOWLEDGMENT

This research was supported by Basic Science Research Program through the National Research Foundation of Korea (NRF) funded by the Ministry of Education (2017R1D1A1A09000590). This work was conducted at High-Speed Compound Unmanned Rotorcraft (HCUR) research laboratory with the support of Agency for Defense Development (ADD).

References

- [1] Hodges, D.H.; Unified approach for accurate and efficient modeling of composite rotor blade dynamics. *Journal of the American Helicopter Society* 2015;60(1):1–28. doi:10.4050/JAHS.60.011001.
- [2] Hodges, D.H.; Nonlinear composite beam the-

ory. Washington, DC: AIAA; 2006. doi:[10.2514/4.866821](https://doi.org/10.2514/4.866821).

- [3] Jung, S.N., Nagaraj, V.T., Chopra, I.; Refined structural model for thin- and thick-walled composite rotor blades. *AIAA Journal* 2002;40(1):105–116. doi:[10.2514/2.1619](https://doi.org/10.2514/2.1619).
- [4] Giavotto, V., Borri, M., Mantegazza, P., Ghiringhelli, G., Carmaschi, V., Maffioli, G.C., et al.; Anisotropic beam theory and applications. *Computers and Structures* 1983;16(1–4):403–413. doi:[10.1016/0045-7949\(83\)90179-7](https://doi.org/10.1016/0045-7949(83)90179-7).
- [5] Cesnik, C.E.S., Hodges, D.H.; VABS: a new concept for composite rotor blade cross-sectional modeling. *Journal of the American Helicopter Society* 1997;42(1):27–38. doi:[10.4050/JAHS.42.27](https://doi.org/10.4050/JAHS.42.27).
- [6] Reissner, E.; On mixed variational formulations in finite elasticity. *Acta Mechanica* 1985;56(3–4):117–125. doi:[10.1007/BF01177113](https://doi.org/10.1007/BF01177113).
- [7] Dhadwal, M.K., Jung, S.N.; Refined sectional analysis with shear center prediction for non-homogeneous anisotropic beams with nonuniform warping. *Meccanica* 2016;51(8):1839–1867. doi:[10.1007/s11012-015-0338-2](https://doi.org/10.1007/s11012-015-0338-2).
- [8] Vlasov, V.Z.; *Thin-walled elastic beams*. Jerusalem: Israel Program for Scientific Translations; 1961.
- [9] Chandra, R., Chopra, I.; Experimental and theoretical analysis of composite I-beams with elastic couplings. *AIAA Journal* 1991;29(12):2197–2206. doi:[10.2514/3.10860](https://doi.org/10.2514/3.10860).
- [10] Chandra, R., Chopra, I.; Structural response of composite beams and blades with elastic couplings. *Composites Engineering* 1992;2(5–7):347–374. doi:[10.1016/0961-9526\(92\)90032-2](https://doi.org/10.1016/0961-9526(92)90032-2).
- [11] Jung, S.N., Park, I.J.; Structural behavior of thin- and thick-walled composite blades with multicell sections. *AIAA Journal* 2005;43(3):572–581. doi:[10.2514/1.12864](https://doi.org/10.2514/1.12864).
- [12] Liu, X., Yu, W.; A novel approach to analyze beam-like composite structures using mechanics of structure genome. *Advances in Engineering Software* 2016;100:238–251. doi:[10.1016/j.advengsoft.2016.08.003](https://doi.org/10.1016/j.advengsoft.2016.08.003).